Eur Biophys J (2011) 40:641–649
DOI 10.1007/s00249-010-0665-0

ORIGINAL PAPER

Effect of Mg^{2+} versus Ca^{2+} on the behavior of Annexin A5 in a membrane-bound state

Zahia Fezoua-Boubegtiten · Bernard Desbat · Alain Brisson · Céline Gounou · Michel Laguerre · Sophie Lecomte

Received: 6 September 2010 / Revised: 26 November 2010 / Accepted: 23 December 2010 / Published online: 25 January 2011

Abstract Annexin A5 (AnxA5) binds to negatively charged phospholipid membranes in a Ca^{2+} dependent manner. Several studies already demonstrate that Mg^{2+} ions cannot induce the binding. In this paper, quartz crystal microbalance with dissipation monitoring (QCM-D), Brewster angle microscopy (BAM), polarization modulation infrared reflection absorption spectroscopy (PMIRRAS) and molecular dynamics (MD) were performed to elucidate the high specificity of Ca^{2+} versus Mg^{2+} on AnxA5 binding to membrane models. In the presence of Ca^{2+}, AnxA5 showed a strong interaction with lipids, the protein is adsorbed mainly in α-helix under the DMPS monolayer, with an orientation of the α-helices axes slightly tilted with respect to the normal of the phospholipid monolayer as revealed by PMIRRAS. The Ca^{2+} ions interact strongly with the phosphate group of the phospholipid monolayer. In the presence of Mg^{2+}, instead of Ca^{2+}, no interaction of AnxA5 with lipids was detected. Molecular dynamics simulations allow us to explain the high specificity of calcium. Ca^{2+} ions are well exposed and surrounded by labile water molecules at the surface of the protein, which then favour their binding to the phosphate group of the membrane, explaining their specificity. To the contrary, Mg^{2+} ions are embedded in the protein structure, with a smaller number of water molecules strongly bound. We conclude that the embedded Mg^{2+} ions inside the AnxA5 structure are not able to link the protein to the phosphate group of the phospholipids for this reason.

Keywords Annexin A5 · Lipid monolayer · Divalent cations · PMIRRAS · Ellipsometry · Molecular dynamics

Abbreviations

AnxA5	Annexin A5
QCM-D	Quartz crystal microbalance with dissipation monitoring
BAM	Brewster angle microscopy
PMIRRAS	Polarization modulation infrared reflection absorption spectroscopy
MD	Molecular dynamics
DMPS	Dimyristoylphosphatidyl-serine

Introduction

Annexins comprise a family of eukaryotic proteins that bind to phospholipid membranes in a Ca^{2+}-dependent manner (Moss 1992). These proteins have been implicated in a variety of membrane-related processes including membrane trafficking, signal transduction, anti-inflammatory activity, and blood coagulation (Gerke and Moss 2002; Greke et al. 2005; Raynal and Pollard 1994). The calcium-dependent membrane binding is thought to play a key role in the cellular functions of annexins, and thus a molecular understanding of this process is an important goal.

Annexin A5 (AnxA5), a 35 kDa hydrophilic molecule with an isoelectric point (pI) of 4.5, is one of several

Electronic supplementary material The online version of this article (doi:10.1007/s00249-010-0665-0) contains supplementary material, which is available to authorized users.

Z. Fezoua-Boubegtiten · B. Desbat · A. Brisson · C. Gounou · M. Laguerre · S. Lecomte (✉)
Laboratoire de Chimie et Biologie des Membranes et des Nano-Objets, UMR 5248 CBMN, CNRS-Université Bordeaux 1-ENITAB, IECB, 2 rue Robert Escarpit, 33607 Pessac, France
e-mail: s.lecomte@cbmn.u-bordeaux.fr

structurally homologous proteins that bind to negatively charged phospholipids, in particular phosphatidylserine lipid (PS), in the presence of Ca^{2+} ions (Meers 1996). The annexins usually contain 4 or 8 domains with about 70 amino acid residues each. Each domain consists of five α-helices, and the four domains are arranged in a cyclic way, giving the molecule an overall flat, slightly curved shape with the Ca^{2+} binding sites located on the convex membrane-binding face (Concha et al. 1993; Huber et al. 1990a, b; Sopkova et al. 1993). The number of calcium sites vary between three and seven, depending on the annexin source (human or rat) and on the calcium concentration (Concha et al. 1993; Huber et al. 1990a, b). Structurally, the Ca^{2+} site in AnxA5 consists of main-chain carbonyl oxygens, carboxylate oxygens of an acidic side chain and water molecules that may occupy the remaining coordination positions. Calcium affinity of annexins in solution is relatively low, becoming higher in the presence of phospholipids (the affinity constants change from millimolar to micromolar). In a previous study, we demonstrated that the phosphate group is the main molecular group involved in the binding of AnxA5 to phospholipids via Ca^{2+} ions, even when some carboxylate groups are accessible (PS) (Fezoua-Boubegtiten et al. 2010). In addition, other types of studies have previously investigated the effect of divalent cations on the AnxA5/phospholipids binding. Andree et al. (Andree et al. 1990) demonstrated that the AnxA5 binding to DOPC/DOPS (20%/80%), bilayers was highly specific for Ca^{2+}, and was also slightly promoted by Cd^{2+}, Zn^{2+}, Mn^{2+}, and Co^{2+} but not by Ba^{2+} and Mg^{2+}. Concha et al. (Concha et al. 1992) also established that calcium was required for the AnxA5-vesicles binding, and magnesium could not substitute for calcium in binding.

Physico-chemical properties of calcium and magnesium ions are close: they both carry the same total apparent charge (+2) and interact with anionic phospholipids such as phosphatidylserine (PS) present at the cellular membrane (Casal et al. 1987, 1989; Dluhy et al. 1983). Moreover, magnesium concentration is higher in the organism than calcium concentration in the organism. The affinity of AnxA5 for divalent cations seems closely related to the size of the divalent ion. The ionic radii of Ca^{2+} and Mg^{2+} are 0.99 and 0.65 Å, respectively (Pauling 1960).

In this study, we investigated the features that may explain the high selectivity of Ca^{2+} ion as a linker between AnxA5 and membranes. We used various approaches to compare the effect of the two ions (Ca^{2+} and Mg^{2+}) on the binding of AnxA5 to a DMPS monolayer at the air–water interface or to supported lipid bilayers (SLBs) (DOPC/DOPS (4:1)). Quartz crystal microbalance with dissipation monitoring (QCM-D) was employed to characterize the adsorption of the protein on SLBs. Brewster Angle Microscopy (BAM) allowed the visualization of the morphology of protein and lipid domains at the air–water interface, as well as changes in lipid monolayer organization after binding of the protein. Ellipsometry measurements were performed to evaluate the thickness of the layers present at the air–water interface. Polarization Modulation Infrared Reflection–Absorption Spectroscopy (PMIRRAS) was carried out to provide direct structural information on the binding of proteins onto phospholipid monolayers. In addition, molecular dynamics simulations were employed to determine the effect of both ions on the dynamics of the AnxA5 structure. We demonstrated that the interaction of AnxA5/phospholipid via cation is strongly depending on the accessibility of the ion on the protein surface to the phosphate group of the lipid.

Materials and methods

Chemicals

Dimyristoylphosphatidylserine (DMPS) was purchased from Sigma. The lipids were dissolved in chloroform/methanol (80%/20% vol./vol.) at 0.2 mg/ml. Organic solvents were purchased from Aldrich (St Quentin Fallavier, France). Ultrapure water with a nominal resistivity of 18 mΩ cm (Milli-Q, Millipore) was used for all buffers and solutions. All other chemicals, of the highest purity available, were purchased from Sigma–Aldrich. Recombinant AnxA5 was produced according to the procedure described by Richter et al. (2005). AnxA5 was stored at 4°C in buffer containing 20 mM Tris/HCl (pH 8.0), 0.02% NaN_3 and 200 mM NaCl.

Preparation of lipid vesicles

Small unilamellar vesicles (SUVs) used in QCM-D experiments were prepared as previously described (Richter et al. 2003). Briefly, a DOPC/DOPS (4:1 w/w) solution was prepared from DOPC and DOPS solutions in chloroform. Lipids were dried under a stream of nitrogen for 2 h and were re-suspended in a buffer containing 150 mM NaCl, 10 mM HEPES, pH 7.4 and 2 mM NaN_3 at a final concentration of 2 mg/ml. The SUVs were obtained by sonication with a tip sonicator (Misonix, Farmingdale, NY) operated in a pulsed mode at 30% duty cycle for 40 min with ice refrigeration, followed by centrifugation in an Eppendorf centrifuge for 10 min at 16,000*g* to remove titanium particles. Lipid concentration was determined by phosphorus content determination (Rouser et al. 1975).

Quartz crystal microbalance with dissipation monitoring (QCM-D)

QCM-D measurements were performed with a Q-SENSE D300 system equipped with an Axial Flow Chamber (QAFC 301) (Q-SENSE AB, Gothenburg, Sweden) (Rodahl et al. 1995). The variations of the resonance frequency (ΔF (Hz)), which are related to the mass of the adsorbed layer, were measured at 25 MHz. The adsorbed mass, m, was calculated according to the Sauerbrey equation, $\Delta m = -C.\ \Delta F$, with $C = 17.7$ ng cm^{-2} Hz^{-1} (Sauerbrey 1959).

Before each experiment, the QCM-D sensor crystals were cleaned in 2% sodium dodecyl sulfate for 10 min, rinsed extensively in ultrapure water, dried under a stream of nitrogen and then treated by UV/ozone for 10 min in a home-made UV/ozone chamber (Richter et al. 2003).

Monolayer formation and surface pressure measurements

Monolayer experiments were performed on a circular Teflon trough (42 cm^2). The surface pressure (π) was measured with a plate of Whatman filter paper held by a Nima Wilhelmy balance. The trough was filled with 8 ml of aqueous buffer containing 10 mM HEPES, 150 mM NaCl, (pH 7.4). An appropriate 2 mM Mg^{2+} or Ca^{2+} solution was added in the buffer solution. The experiments of AnxA5 under the lipid monolayers were carried out at 26 ± 2°C. The interaction of AnxA5 with DMPS films was performed in two steps. In the first step, the lipids were spread at the air–water interface from chloroform/methanol (80%/20% vol./vol.) solutions using a Hamilton microsyringe to reach a surface pressure of 30 mN/m. In the second step, multiple injections of few microliters of the AnxA5 stock solution were performed into the subphase and the surface pressure was recorded for each protein concentration (from 29 to 200 nM).

PMIRRAS spectroscopy

PMIRRAS spectra were recorded on a Nicolet (Madison, WI) Nexus 870 spectrometer equipped with a liquid-nitrogen-cooled mercury cadmium telluride (MCT) detector (SAT, Poitiers) at 77 K with a resolution of 8 cm^{-1}. Six hundred scans representing an accumulation time of 10 min were collected for each spectrum of the AnxA5/DMPS monolayers. The optimal value of the angle of incidence for the detection was 75° relative to the optical axis normal to the interface. At this angle of incidence, a negative band indicated a transition dipole moment oriented preferentially perpendicular to the surface, whereas a positive reflection adsorption band was related to a transition dipole moment oriented preferentially in the plane of the surface (Blaudez et al. 1996). For the AnxA5/DMPS monolayer experiments, the PMIRRAS spectra of the AnxA5 shown were normalized by the lipid spectrum. These spectra allowed us to extract the characteristic contributions of the protein and to detect only the changes in the lipid head groups and acyl chains vibrations induced by the binding of AnxA5 to the lipid monolayers.

Brewster angle microscopy (BAM) and ellipsometry measurements

BAM images were recorded using a NFT Ielli 2000 Brewster angle microscope (Göttingen, Germany) equipped with a doubled frequency Nd-Yag laser (532 nm, 50 mW), a polarizer, an analyzer and a CCD camera. The lateral resolution of the BAM images (570 × 450 μm) with the ×10 magnification lens was about 2 μm, and the BAM images were coded in gray level. From the reflectance value, the BAM thickness model allows evaluation of the thickness of the layer at the surface with the knowledge of the experimental Brewster angle and the optical index of the film (De Mul and Mann 1998). For ellipsometric measurements, one compensated plate was added to the same setup of BAM microscopy. Most of the ellipsometric measurements were done with an incidence angle close to the Brewster angle (52°). The imaging ellipsometer operates on the principle of classical null ellipsometry (Azzam and Bashara 1977). The polarizer, compensator, and analyzer angles which give the null condition for one sample allow the (Δ, Ψ) ellipsometric angles related to the optical properties of this sample to be calculated. For ultrathin film, the variation of $\boldsymbol{\Delta}$ angle ($\delta\Delta$) is proportional to the film thickness. We used a refractive index of 1.45 to determine the thickness value of the phospholipid and the complex AnxA5/phospholipid, as justified in our previous paper (Fezoua-Boubegtiten et al. 2010).

Molecular dynamics (MD)

We carried out several molecular dynamics simulations using NAMD (Phillips et al. 2005) software v2.6 and CHARMM 27 force-field. All simulations were performed on a 32 processor IBM PC-cluster using 8 to 16 processors. The simulation boxes were built using VMD v1.8.6 facilities. All images were captured from VMD (Humphrey et al. 1996) using Tachyon internal ray-tracing software. In all cases, molecular dynamics runs were performed with periodic boundary conditions at constant pressure (1 bar) using the modified Nosé-Hoover Langevin method implemented in NAMD: the target pressure was 1 bar, the oscillation period of the Langevin piston was 200 fs and the Langevin piston damping time scale

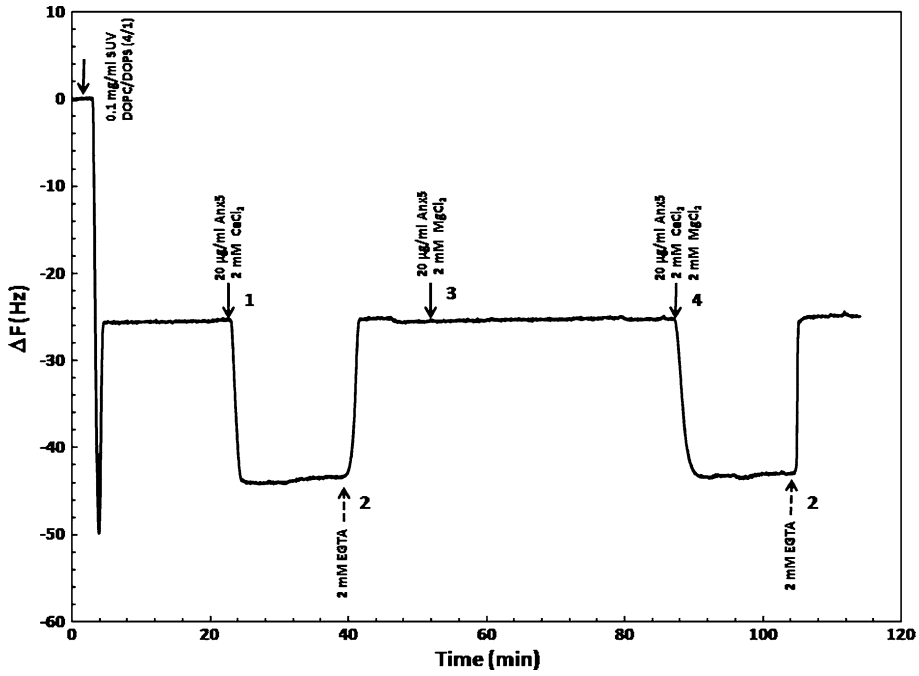

Fig. 1 QCM-D response (frequency, ΔF) at 25 MHz. The SLB was formed by incubation of SUVs of DOPC/DOPS (4:1w/w) on silica (0 min). The adsorption of annexin A5 (injections indicated by *solid arrows*) was measured in the presence of 2 mM $CaCl_2$ (*arrow* 1), 2 mM $MgCl_2$ (*arrow* 3) and both 2 mM $CaCl_2$ and 2 mM $MgCl_2$ (*arrow 4*). *Dotted arrow* 2 indicates rinses in a buffer solution containing 2 mM EGTA

was 100 fs. We used throughout a multiple time step integration with 1 fs for bonded forces and 4 fs for long range electrostatic forces. Electrostatic interactions were treated using Particle Mesh Ewald (PME) with a cubic grid of 96 points on each dimension. The Van der Waals (VDW) cut-off was set at 1 nm with 20 time steps for each reassignment cycle. SHAKE protocol was on but only on water hydrogens.

The whole complex was immersed in a box of water, fully ionized with all protein charges neutralized by counter ions. Two models were built: without added salts and with 4 metal atoms (calcium or magnesium) located according to the PDB structure code 1ANX (resolution 2 Å) of the human Annexin V (Huber et al. 1990a). Two other models identical to the preceding ones were built with added salts corresponding to a final 150 mM NaCl concentration (physiological concentration). Model 1 was built with 4 calcium, without added salts, and totaled 54.741 atoms with 16.577 water molecules (TIP3P). Model 2 used 4 magnesium, without added salts, and totaled 54.741 atoms with 16.577 water molecules (TIP3P). Model 3 used 4 calcium and added salts, and totaled 54.555 atoms with 16.484 water molecules (TIP3P). Model 4 used 4 magnesium and added salts, and totaled 54.555 atoms with 16.484 water molecules (TIP3P). These systems were constructed in a box of $106.40 \times 71.26 \times 76.72$ $Å^3$, at $T = 300$ K and $P = 1$ bar. In each case the examined time simulation was 10 ns. Finally, Model 5 was built including Annexin A5 alone, without any added salts or calcium and magnesium ions, except 11 sodium ions to fully neutralize the system (the model includes 19,781 water molecules). This Model was run for 20 ns.

Results and discussion

Adsorption of annexin A5 on SLBs in the presence of Ca^{2+} or Mg^{2+} ions

Figure 1 shows QCM-D response of adsorption of AnxA5 to a DOPC/DOPS (4:1) supported lipid bilayers in the presence of 2 mM $CaCl_2$ or $MgCl_2$. We confirmed existing knowledge that Mg^{2+} does not promote AnxA5 binding (Richter et al. 2005). We also demonstrated that addition of Ca^{2+} in buffer containing Mg^{2+} restores the AnxA5 binding (Fig 1. Arrow 4). Thus, Mg^{2+} neither induces nor prevents AnxA5 binding to membrane containing PS.

Structure and orientation of AnxA5 interacting with a DMPS monolayer in the presence of Ca^{2+} or Mg^{2+} ions

BAM images presented in Fig. 2 show that only in the presence of Ca^{2+} an increase of the average reflectance level up to 9.89×10^{-6} is observed, compared with DMPS monolayer alone ($R = 2.38 \times 10^{-6}$), as expected. No domain appears at the spatial resolution of the Brewster angle microscope. The thickness of the AnxA5/Ca^{2+}/DMPS film at 27 mN/m was estimated from BAM and ellipsometry ($\delta\Delta = 23.7°$) measurements at 52 ± 2 and

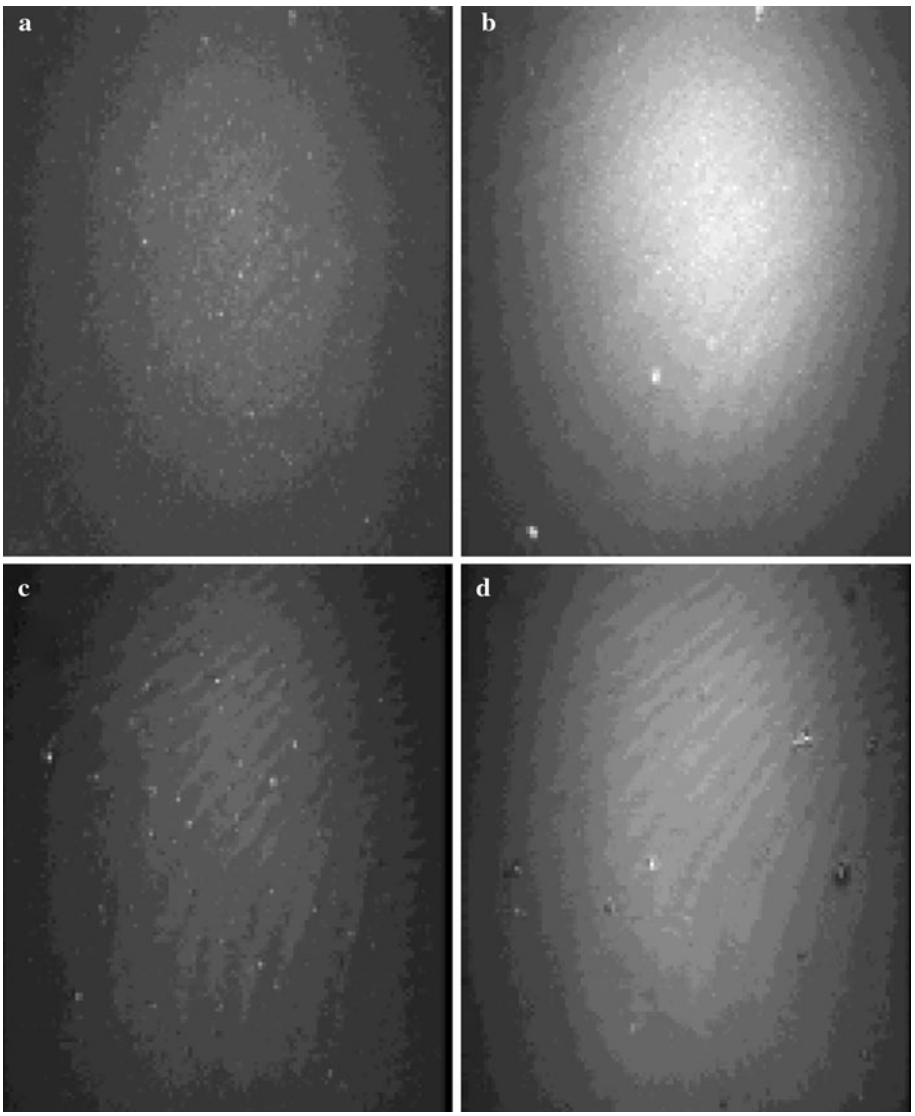

Fig. 2 BAM images (570 × 450) μm of a DMPS monolayer with 2 mM $CaCl_2$: **a** without AnxA5 (t = 33 min, π = 30.6 mN/m, R = 2.38 × 10^{-6}); **b** with 148 nM AnxA5 (t = 2 h 47 min, π = 27.8 mN/m, R = 9.89 × 10^{-6}). BAM images of a DMPS monolayer with 2 mM $MgCl_2$: **c** with 160 nM AnxA5 (t = 3 h 53 min, π = 27.3 mN/m, R = 2.76 × 10^{-6}); and **d** with 2 mM $CaCl_2$ added to the subphase of AnxA5/Mg^{2+} layer (π = 23 mN/m, R = 0.98 × 10^{-5})

55 ± 2 Å, respectively, using a refractive index of 1.45. The thickness of the DMPS monolayer was calculated at 20 Å, and then the thickness of the AnxA5 layer under the DMPS monolayer was estimated at 35 Å. In the presence of Mg^{2+}, the BAM image recorded after injection of AnxA5 under DMPS monolayer (Fig. 2c) is similar to the BAM image of the DMPS alone (Fig. 2a). Thus, no effective binding of the AnxA5 to DMPS monolayer takes place in the presence of Mg^{2+}, as expected. In order to investigate the calcium specificity of AnxA5 binding to DMPS, we injected 2 mM $CaCl_2$ solution beneath the AnxA5/Mg^{2+}/DMPS mixture. The BAM image registered at the final state of AnxA5 adsorption displays a condensed homogeneous film (Fig. 2d). The film thickness obtained from experimental ellipsometric signal ($\delta\Delta$ = 22.3°) is 52 (±2) Å, which is similar to the BAM estimation 51 (±2) Å, which is close to the thickness of AnxA5/Ca^{2+}/DMPS film (55 Å). It is noteworthy that the binding of AnxA5 to the phospholipid monolayer is restored with addition of calcium. This observation further stresses that the cation requirement for Anx5 binding to phospholipid is highly specific for Ca^{2+} as already observed by Andree et al. (Andree et al. 1990).

First, we evaluated the effect of Ca^{2+} or Mg^{2+} ion on DMPS monolayer, by PMIRRAS (see Supplementary material Fig. S1). The hydrated antisymmetric PO_2^- vibration of the DMPS monolayer without ion gives an intense band observed at 1219 cm^{-1}. Addition of 2 mM Ca^{2+} or Mg^{2+} induces a shift of this band to 1225 and 1222 cm^{-1}, respectively. Thus, the phosphate group of the DMPS interacting with Ca^{2+} or Mg^{2+} is less hydrated in the presence of both ions. Figure 3 shows the normalized PMIRRAS spectra of AnxA5 under DMPS monolayer in the presence of Ca^{2+} (Fig. 3a), Mg^{2+} (Fig. 3b) and Mg^{2+}

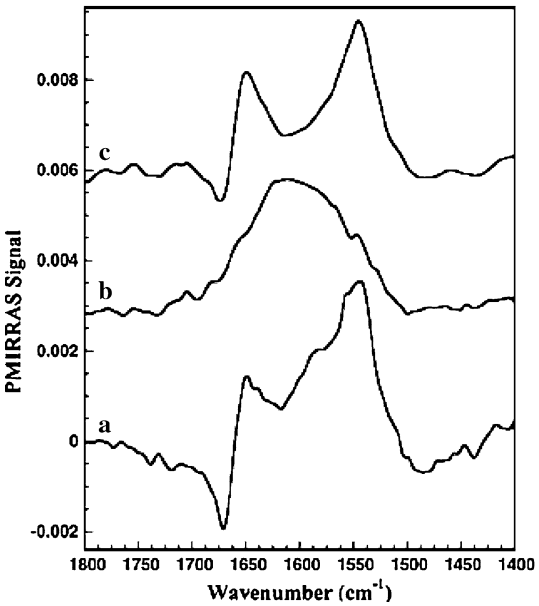

Fig. 3 PMIRRAS spectra of AnxA5 in interaction with a DMPS monolayer ($\pi = 30$ mN/m): **a** in the presence of 2 mM $CaCl_2$ (120 nM AnxA5, $\pi = 26.8$ mN/m); **b** in the presence of 2 mM $MgCl_2$ (160 nM AnxA5, $\pi = 27.1$ mN/m); and **c** after injection of 2 mM $CaCl_2$ to the subphase under AnxA5/Mg^{2+}/DMPS mixture. Subphase: HEPES buffer 10 mM, 150 mM NaCl, pH 7.4—T = 26°C

with addition of Ca^{2+} (Fig. 3c). Binding of AnxA5 to a DMPS monolayer in the presence of Ca^{2+} is proven by the presence and high intensity of the amide I and amide II bands (Fig. 3a). This binding induces no perturbation of the ester group of the lipid, as revealed by the disappearance of this lipid vibration on the AnxA5 spectra normalized by the DMPS spectrum (see "Material and methods"). The dispersive-like shape of amide I band with a positive band centered at 1653 cm^{-1} and an intense amide II band reveal that AnxA5 maintains its α-helix structure. According to the previous simulation of the normalized PMIRRAS spectra of pure α-helices (Blaudez et al. 1996; Buffeteau et al. 1999; Cornut et al. 1996; Lavoie et al. 1999), the amide I/amide II ratio (AI/AII) was used to estimate the relative orientation of the α-helices. Thus, the AI/AII ratio of 0.7 obtained for the AnxA5 under DMPS indicate an average orientation of 30° of the α-helices axes with respect to the normal to the interface. In the presence of Mg^{2+} instead of Ca^{2+}, there is no evidence of binding of the protein to the DMPS, as already demonstrated by ellipsometry and QCM-D experiments. A large band in the 1500–1700 cm^{-1} range was observed (Fig. 3b) and pointed out a perturbation of both the carboxylate antisymmetric vibrations $\nu_{as}(COO^-)$ of the serine head group of DMPS, and the water molecular layer under DMPS monolayer. Thus, no organization of AnxA5 under the DMPS monolayer can occur in the presence of Mg^{2+}. Finally, addition of 2 mM Ca^{2+} beneath the AnxA5/Mg^{2+}/DMPS mixture

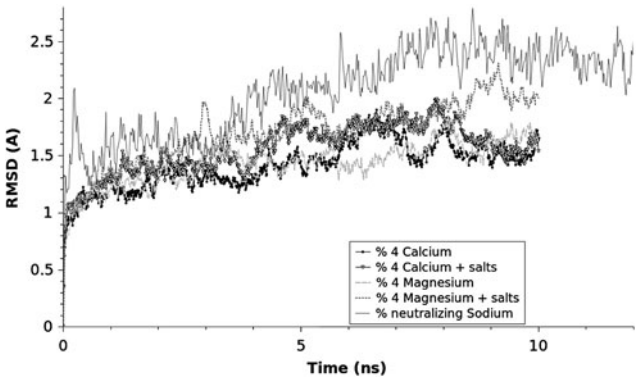

Fig. 4 Plot of root mean square deviation (RMSD) values (Å) obtained during the five molecular dynamics runs as a function of time of simulation

leads to the binding of AnxA5 under the DMPS monolayer (Fig. 3c). Thus, the profiles of the amide I and amide II bands are similar to the PMIRRAS spectrum of AnxA5 in AnxA5/Ca^{2+}/DMPS complex (Fig. 3c). Consequently, the same orientation of α-helices (slightly tilted with respect to the normal to the phospholipid monolayer) is assumed for AnxA5 in a lipid environment after injection of Ca^{2+}. Our results clearly demonstrate that only Ca^{2+} ions are able to promote the binding of AnxA5 to the phospholipid monolayer. In a previous paper, we demonstrated that Ca^{2+} ions linked the phosphate group of the lipid to the AnxA5 protein (Fezoua-Boubegtiten et al. 2010). Herein, we established that the binding of ion (Ca^{2+} or Mg^{2+}) to DMPS is similar, but the protein-lipid binding occurs only in the presence of Ca^{2+}, leading to the specific effect of Ca^{2+} on the AnxA5 organization.

Molecular dynamics of AnxA5: effect of Ca^{2+} or Mg^{2+} ions

Molecular Dynamics (MD) simulations of crystallized AnxA5 with calcium and magnesium ions (Ca^{2+} or Mg^{2+}) in an aqueous medium were performed to carry out the effect of each ion on the stability of AnxA5. The main difference between Ca^{2+} and Mg^{2+} is the smaller ionic radius of the magnesium. The charge density of both ions is 1.55 $e^-/Å^3$ for Ca^{2+} and 5.22 $e^-/Å^3$ for Mg^{2+} respectively, which is significantly different.

MD simulations of AnxA5 with divalent cations in the different models (see Materials and Methods part) exhibit, on the whole, a very high stability within the examined time frame (see Fig. 4). The maximum value of RMSD (root mean square deviation), reached during the four molecular dynamics runs with divalent ions, is 2.3 Å for AnxA5 without divalent ions, with an average around 1.7–1.8 Å during the last 5 ns. These results show that AnxA5 undergoes no modification in structure when replacing calcium by

magnesium. The presence of divalent cations seems to be largely favorable to the stability of secondary structures. In the presence either of Ca^{2+} or Mg^{2+}, a careful survey of the secondary structure *versus* time (Fig. 5a, b) leads to the conclusion that the secondary structure (and mainly the length of the α-helices) is extremely stable: no fluctuation can be observed during the entire simulation run. On the contrary, when divalent cations are absent (Model 5) and even if the global RMSD is not very high (2.3 ± 0.4 Å during the last 10 ns, Fig. 4) the plot of secondary structure *versus* time (Fig. 5c) shows large fluctuations. Then, structures of α-helices display a large number of short interruptions compared to the divalent cations plots (Fig. 5a, b). It is clear that in the absence of these divalent cations the whole structure of Annexin A5 experiences large fluctuations. Results obtained for AnxA5 in solution without and with divalent ions probed by ATR-FTIR spectroscopy are in agreement with the MD simulations. These results are detailed in Supplementary material (see results, Fig. S2 and Table S1). The structure of AnxA5 in solution exhibits more flexibility in the absence of ion than in the crystal form. Indeed, the percentage of amide I group corresponding to α-helice structures (71%) is lower than in the crystallized form (80%). Only addition of Ca^{2+} promotes a high organization of AnxA5 in solution with a high percentage of α-helice structures.

To perform MD simulation with Mg^{2+} ion, well located Ca^{2+} were replaced by Mg^{2+} ions without other modifications. When looking at the hydration sphere around each of the four conserved metal positions, the result is completely different from calcium to magnesium on the AnxA5 (Fig. 6), the average distance between adjacent metal ions being respectively 9–12 Å and 11–14 Å. The consequence is that one water molecule cannot belong to more than one first hydration sphere (radius less than 4 Å). In these conditions, the total number of bound water molecules is around 14 with calcium (with and without added salts, Fig. 6a, b) and only 7.0 with magnesium (Fig. 6c, d). As a consequence, the magnesium atoms are dramatically less accessible to water, and half of them are completely embedded within the protein structure, having almost no contact with the exterior environment (Fig. 7). The four Ca^{2+} ions are located just outside the protein surface being fully accessible to water (Fig. 7a, b). In the case of Mg^{2+} ions, the two more external ions are not visible when the protein surface is drawn and the remaining two ions are less solvated compared to the calcium models (Fig. 7c, d). This is very obvious when comparing the calcium model with the high magnesium content (Fig.S3 in Supplementary material). Thus, the poor binding of AnxA5 to membrane in the presence of high concentration of Mg^{2+} can be explained by the lack of accessibility of the embedded ion to the phosphate group of the lipid. Moreover, the phosphate groups of the lipids, which are stronger negative groups than carboxylate groups, also strongly bind to the magnesium ions of the solution creating a fixed positive charged layer under the negative charged lipids repulsive against the Annexin-Mg complex.

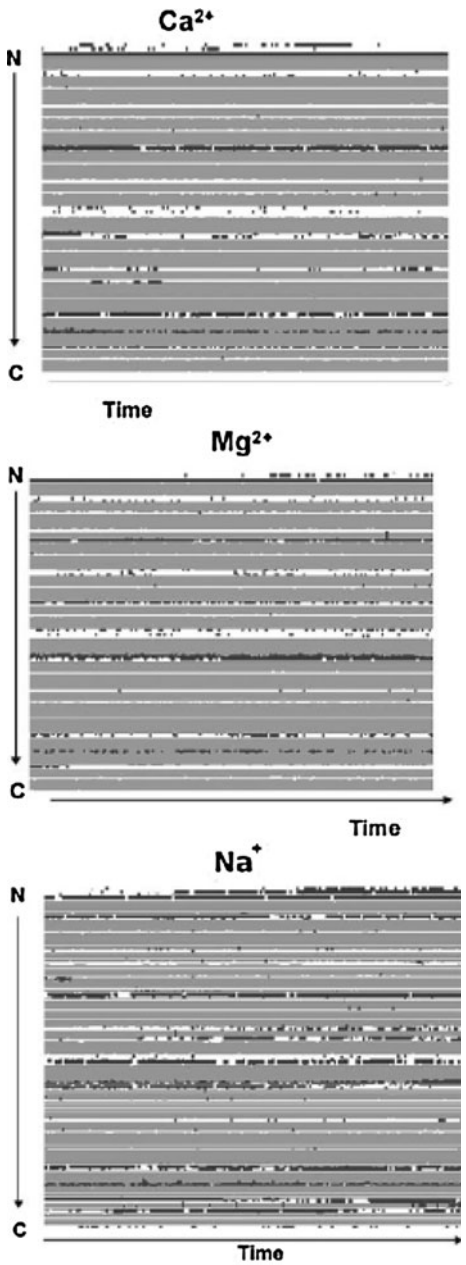

Fig. 5 Timeline plots of secondary structure (Y axis) *versus* simulation time (X axis) of Anx A5. α-helices are depicted in grey, turns in *black* and random structures in *white*. Top for Model 1 (four Ca^{2+} and no added salts), middle for Model 2 (four Mg^{2+} and no added salts) and bottom Model 5 (no added salts and only Na^{+} ions for neutralization purpose). In the *upper plots* the *grey bars* representing the alpha-helices are extremely stable during simulation times. Note in the bottom plot the presence of numerous *white lines* within the *grey bars*, which are absent in the two upper plots and indicating short interruptions of the α-helix structures. Note also the more obvious presence of *black dots* in the bottom plot as a consequence of more turns within the whole structure

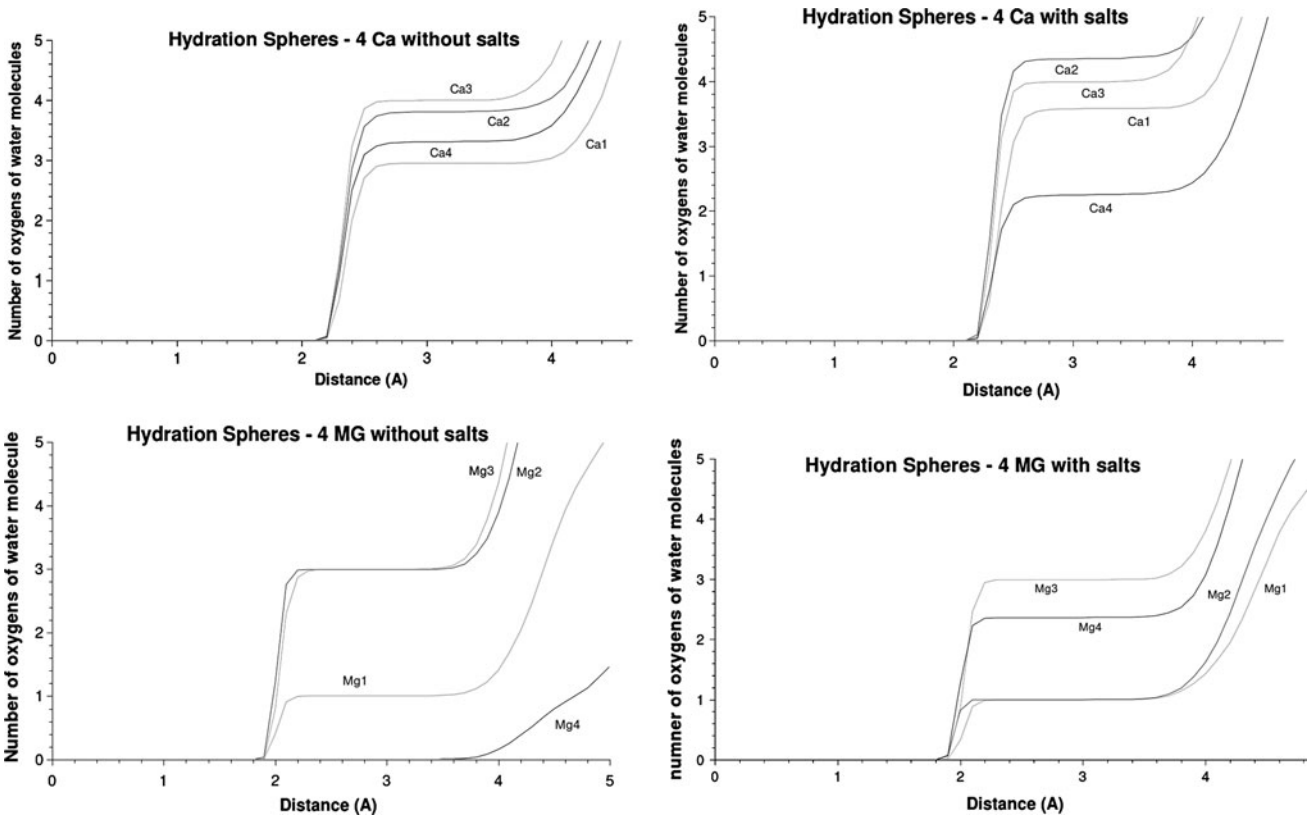

Fig. 6 Radial distribution function of water oxygens around each metal ions, only for the four conserved ion positions. Note that a water molecule cannot belong to more than one first hydration sphere due to the average distance between adjacent metal ions (9–12 and 11–14 Å, respectively)

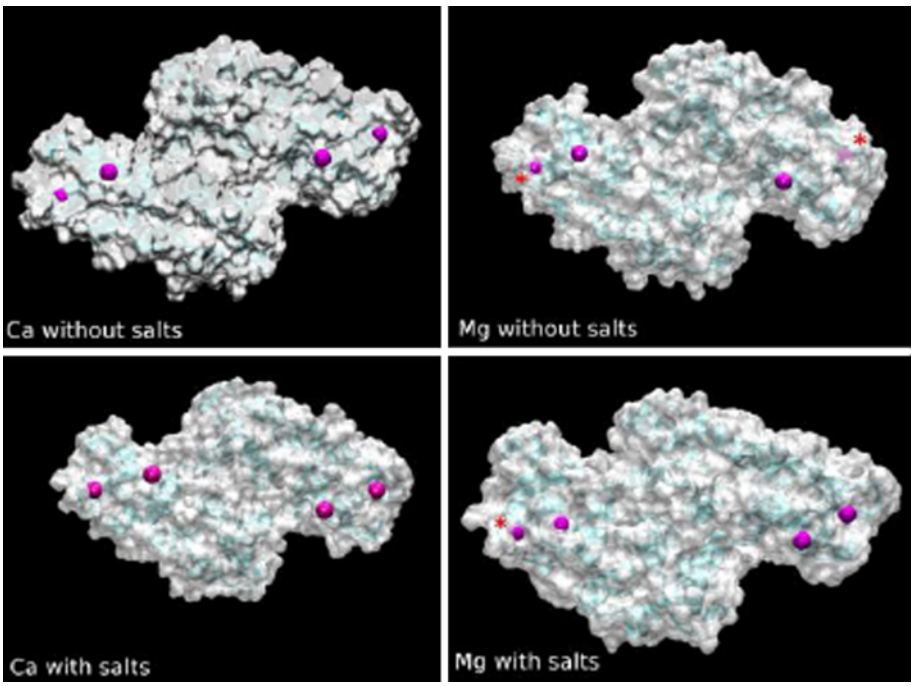

Fig. 7 Four models with the protein surface in a glassy surface and the structure as a *blue ribbon*. Metal ions are shown as magenta VdW spheres. *Red stars* show the surface embedded ions

Conclusion

Our findings emphasize that in the absence of Ca^{2+}, and also in the presence of Mg^{2+}, no binding of AnxA5 to membrane models was detected. In the presence of Ca^{2+}, PMIRRAS experiments showed that AnxA5 is adsorbed mainly in α-helix structures under the DMPS monolayer. The α-helices axes are oriented rather perpendicular with respect to the normal to the interface. After addition of Ca^{2+} to the AnxA5/Mg^{2+}/DMPS mixture the AnxA5 regains its preferential conformation (α-helix structures) and orientation under the DMPS monolayer. This specificity for Ca^{2+} to mediate annexin binding to membranes may be of the biological relevance, particularly for the cellular functions of annexins. MD simulations of AnxA5 structure with calcium and magnesium ions pointed out that the calcium ions are fully accessible to water on the AnxA5 surface, whereas half of the magnesium ions are totally embedded inside the protein structure. This supports the strong membrane-binding specificity of AnxA5 for calcium that links the protein to the phosphate group of lipid, and further stress that the protein does not bind to the membrane, in the presence of magnesium. The embedded positions of Mg^{2+} prevent binding to the membrane.

Acknowledgments Z. F–B received a fellowship from the French Ministry of research.

References

Andree HAM, Reutelingsperger CPM, Hauptman R, Hemker HC, Hermens WT, Willems GM (1990) Binding of vascular anticoagulant alpha (VAC alpha) to planar phospholipid bilayer. J Biol Chem 265:4923–4928

Azzam RMA, Bashara NM (1977) Ellipsometry and polarized light. Physics publishing New York, North Holland

Blaudez D, Turlet JM, Dufourcq J, Bard D, Buffeteau T, Desbat B (1996) Investigation at air-water interface using polarization modulation IR spectroscopy. J.Chem Soc Faraday Trans 92:525–530

Buffeteau T, Blaudez D, Péré E, Desbat B (1999) Optical constant determination in the infrared on uniaxially oriented monolayers from transmittance and reflectance measurements. J Phys Chem B 103:5020–5027

Casal HL, Mantsch HH, Hauser H (1987) Infrared studies of fully hydrated saturated phosphatidylserine bilayers: effect of Li^{+} and Ca^{2+}. Biochemistry 26:4408–4416

Casal HL, Mantsch HH, Hauser H (1989) Infrared and ^{31}P-NMR studies of interaction of Mg^{2+} with phosphatidylserines : effect of hydrocarbon chain unsaturation. Biochim. Biophys. Acta Biomembranes 982:228–236

Concha NO, Head JF, Kaetzel MA, Dedman JR, Seaton BA (1992) Annexin V forms calcium-dependent trimeric units on phospholipid vesicles. FEBS Lett. 314:159–162

Concha NO, Head JF, Kaetzel MA, Dedman JR, Seaton BA (1993) Rat annexin V crystal structure: Ca^{2+}—induced conformational changes. Science 261:1321–1324

Cornut I, Desbat B, Turlet JM, Dufourcq J (1996) In situ study by polarization modulated Fourier transform infrared spectroscopy of the structure and orientation of lipids and amphipatic peptides at air-water interface. Biophys J 70:305–312

De Mul MNG, Mann JA (1998) Determination of the thickness and optical properties film from the domain morphology by Brewster angle microscopy. Langmuir 14:2455–2466

Dluhy RA, Cameron DG, Mantsch HH, Mendelsohn R (1983) Fourier transform infrared spectroscopic studies of the effect of calcium ions on phosphatidylserine. Biochemistry 22:6318–6325

Fezoua-Boubegtiten Z, Desbat B, Brisson A, Lecomte S (2010) Determination of molecular groups involved in the interaction of Annexin A5 with lipid membrane models at the air-water interface. Biochim Biophys Acta Biomembranes 1798:1204–1211

Gerke V, Moss SE (2002) Annexins : from structure to function. Physiol Rev 82:331–371

Greke V, Creutz CE, Moss SE (2005) Annexins: linking ca2 + signalling to membrane dynamics. Nat Rev Mol Cell Biol 6:449–461

Huber R, Römisch J, Paques EP (1990a) The crystal and molecular structure of human annexin V, an anticoagulant protein that binds to calcium and membranes. EMBO J 9:3867–3874

Huber R, Schneider M, Mayr I, Römisch JM, Paques EP (1990b) The calcium binding sites in human annexin V by crystal structure analysis at 2.0 A resolution. Implications for membrane binding and calcium channel activity. FEBS Lett 275:15–21

Humphrey W, Dalke A, Schulten K (1996) VMD-Visual molecular dynamics. J Mol Graph 14:33–38

Lavoie H, Gallant J, Grandbois M, Blaudez D, Desbat B, Boucher F, Salesse C (1999) The behaviour of membrane proteins in proteins in monolayers at the gas-water interface: Comparison between photosystem II, rhodopsin and bacteriorhodopsin. Mat Sci Eng C-Bio S 10:147–154

Meers P (1996) Annexin binding to lipid assemblies In: Seaton BA (ed) Annexins: molecular structure to cellular function. R. G. Landes Company, Austin, pp 97–119

Moss E (1992) The annexins. Portland Press, London

Pauling L (1960) The nature of the chemical bond. Cornell university press, Ithaca

Phillips JC, Braun R, Wang W, Gumbart J, Tajkhorshid E, Villa E, Chipot C, Skeel RD, Kale L, Schulten K (2005) Scalable molecular dynamics with NAMD. J Comput Chem 26:1781–1802

Raynal P, Pollard HB (1994) Annexins: the problem of assessing the biological role for a gene family of multifunctional calcium-and phospholipid-binding proteins. Biochim Biophys Acta 1197: 63–93

Richter RP, Mukhopadhyay A, Brisson A (2003) Pathways of lipid vesicle deposition on solid surfaces: a combined QCM-D and AFM study. Biophys J 85:3035–3047

Richter RP, Lai Kee Him J, Tessier B, Tessier C, Brisson AR (2005) On the kinetics of adsorption and two-dimensional self-assembly of annexin A5 on supported lipid bilayers. Biophys J 89:3372–3385

Rodahl M, Höök F, Krozer A, Brzezinski P, Kasemo B (1995) Quartz crystal microbalance setup for frequency and Q-factor measurements in gaseous and liquid environments. Rev Sci Instrum 66:3924–3930

Rouser G, Fleisher S, Yamamoto A (1975) Two dimensional thin layer chromatographic separation of polar lipids and determination of phospholipids by phosphorus analysis of spots. Lipids 5:494–496

Sauerbrey G (1959) Verwendung von Scwingquartzen zur Wagung dunner Schinchten und zur Mikrowagung. Z Phys 155:206–222

Sopkova J, Renouard M, Lewit-Bently A (1993) The crystal structure of a new high-calcium form of annexin V. J Mol Biol 234:816–825